Thermo-mechanical Analysis of Parts Fabricated via Fused Deposition Modeling (FDM)

Manish Bharvirkar, Phong Nguyen, Christoph Pistor (Ph.D.)
University of Utah

Abstract:

The quality of Fused Deposition Modeling parts that are built using the standard parallel road approach depends significantly on the orientation of the slices. In this study the expansion coefficient, tensile strength and elastic modulus of FDM parts made from ABS were determined experimentally. The parts were built using the standard toolpath (parallel roads) with a uni directional stacking sequence. The results were used to determine the thermo-mechanical properties for an individual slice. Classical lamination theory was applied to predict properties and stiffness matrix of parts with arbitrarily oriented stacking sequences. The results of these predictions are compared with experimental results for a quasi-isotropic stacking sequence.

Introduction:

Part Quality of FDM parts mainly relates to part strength, surface quality and dimensional accuracy. FDM parts are produced by extruding material and depositing it in layers. This result in poorer mechanical properties within a layer due to the formation of interbead interfaces and voids coupled with the inherent isotropic nature of extruded roads. Therefore, it is important to select a good orientation to achieve better strength. This paper shows how orientation, that is, the orientation of the part and orientation of roads within individual slices influences part strength. It will be also shown how various orientations affect the coefficient of thermal expansion of the part.

Thermal Expansion Experiment:

In order to identify the thermal expansion coefficients of parts built with the Fused Deposition process, three mutually orthogonal oriented specimens (see Figure 1) were made for two different stacking sequences. The xy-plane is the build plane of the machine. The stacking sequence of the roads was chosen to represent a uni-directional and a quasi-isotropic laminate [0 90 45 -45]. This resulted in a total of 20 layers for the specimen built in the xy plane and a total of 197 layers for the specimen built in the yz- and xz-plane.

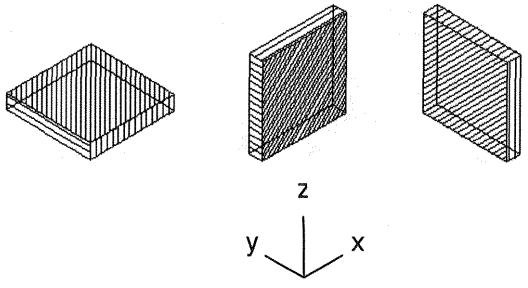

Figure 1: Sample Orientation for Thermal Expansion Measurements

These ABS parts were built using default parameters in QuickSlice 5.0. For the parts built in xy-plane, the top surface was chosen for strain-gage installation whereas no such preference was given for the remaining samples. The surfaces of the specimens were sanded to obtain a good bonding with strain gages. Standard 120 Ω strain-gages with a gage factor of 2 and M2000 Bond were used. Strain-gage installation was performed according to the gage manufacturer's specification [4].

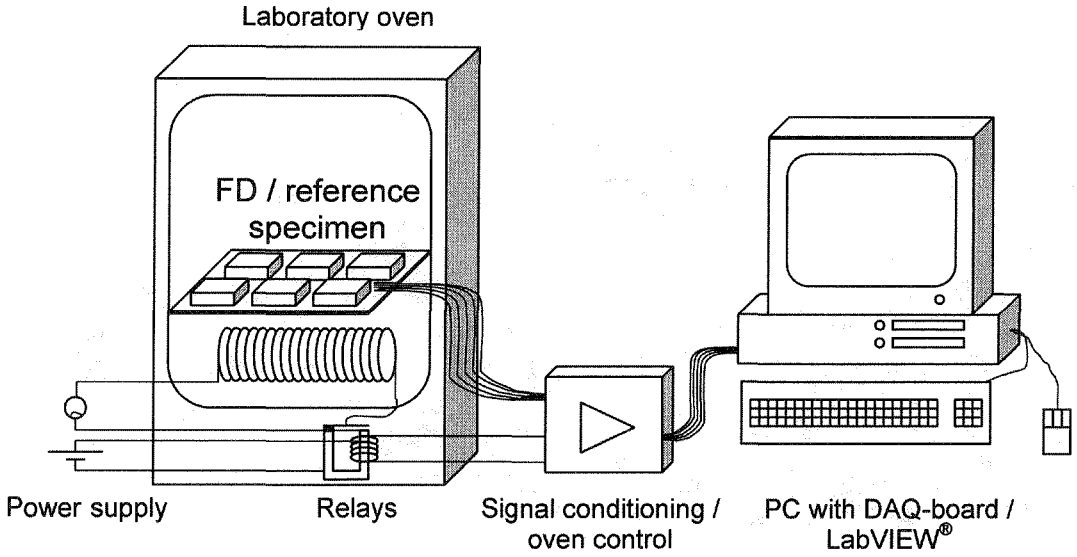

Figure 2: Experimental set-up for thermal expansion measurements

See Figure 2 for experimental set-up. It consists of a laboratory oven that is controllable with a transistor / relays arrangement connected to a digital output of the data acquisition (DAQ) board. Specific software modules for calibration were implemented in LabVIEW® and allow the temperature for the expansion measurements to follow a preset heating and cooling rate. Three Fused Deposition (FD) specimen and three glass reference specimens were placed simultaneously inside the oven with strain gages and thermocouples attached. Three half-bridge circuits (Figure 3) one for each pair of FD and glass reference specimen, were included in the signal conditioning box. The three bridge signals are then amplified using three precision signal integrated circuit amplifiers AD624 (Analog Devices, [2]). The K-type thermocouples are amplified using AD594 (Analog Devices, [1]) amplifiers that include thermocouple signal calibration and cold junction compensation.

The architecture of the half-bridge circuit, the experimental procedure, and the determination of the thermal strain are described in (Measurement Group, [4]). The circuit diagram for strain measurement is as shown in Figure 3. To account for the expansion of the gage and the adhesive, a second gage is used which is bonded to a reference material. The reference material was chosen to be Borosilicate Glass with a known expansion coefficient of $32.5*10^{-7}$ [m/m-K].

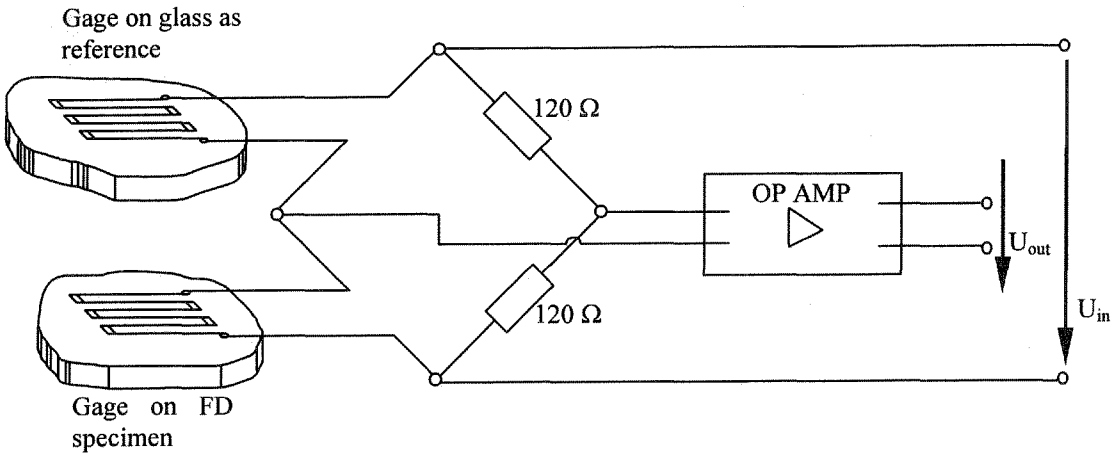

Figure 3: Half bridge circuit for strain measurements

In each experiment the specimens were placed inside the laboratory oven on a glass plate, to reduce friction during expansion. The LabVIEW® program controls the heating rate so that the temperature is increased linearly upto 100 °C and then decreased back to room temperature. The strains and temperatures of all FD specimens were recorded at a rate of one sample per minute. Figures 4 shows typical plots as obtained from the experiment .

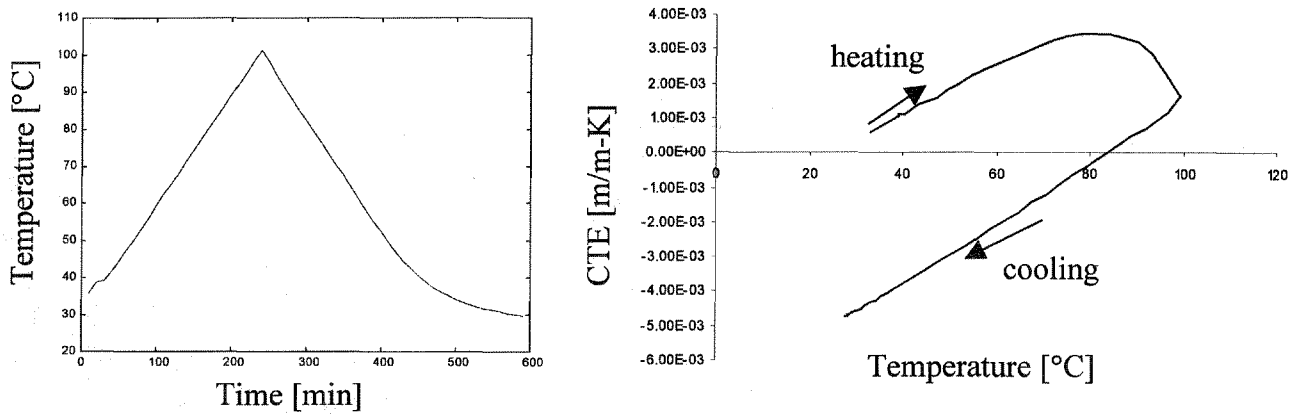

Figure 4: Temperature History (left) and Coefficient of thermal expansion (right) during Thermal Expansion Measurement

Tensile tests of uni-directional specimens:

Tensile tests were carried out on 7 specimens (designed according to ASTM D 5937-96 standard) to calculate the effective moduli of uni-directional (corresponding to continuous fiber-reinforced laminae) bars. Young's modulus was obtained from the stress-strain diagram for bars labeled 1,2 and 3 as follows:

$$E_x = \frac{\Delta\sigma_x}{\Delta\varepsilon_x}$$

The longitudinal and the transverse strain are recorded using strain-gages and a data acquisition system. The Poisson ratio was obtained from data acquired by the DAQ board and is given as:

$$\nu_{xy} = -\frac{\varepsilon_y}{\varepsilon_x}$$

Shear Modulus was obtained from the test of bars labeled 4,5 and 6, as follows:

$$G_{ab} = \frac{E_x}{2(1+\nu_{xy})}$$

where x and y are the direction of load application and the transverse direction respectively. Also, a and b correspond to 1 and 2 for the specimen in the xy plane, 2 and 3 for the specimen in the xz plane, for and 3 and 1 for the one in yz plane.

Similar to linear and elastic composites, it is assumed that reciprocity relation holds for FDM parts. As a result the compliance matrix, and therefore the stiffness matrix, is symmetric. The complete stiffness matrix is given as follows:

$$[S]=\begin{bmatrix} \frac{(1-\nu_{23}\nu_{32})E_1}{1-\nu} & \frac{(\nu_{21}+\nu_{31}\nu_{23})E_1}{1-\nu} & \frac{(\nu_{31}+\nu_{21}\nu_{32})E_1}{1-\nu} & 0 & 0 & 0 \\ & \frac{(1-\nu_{13}\nu_{31})E_2}{1-\nu} & \frac{(\nu_{32}+\nu_{12}\nu_{31})E_2}{1-\nu} & 0 & 0 & 0 \\ & & \frac{(1-\nu_{12}\nu_{21})E_3}{1-\nu} & 0 & 0 & 0 \\ & \text{sym.} & & G_{23} & 0 & 0 \\ & & & & G_{13} & 0 \\ & & & & & G_{12} \end{bmatrix}$$

where $\nu = \nu_{12}\nu_{21} + \nu_{23}\nu_{32} + \nu_{31}\nu_{13} + 2\nu_{21}\nu_{32}\nu_{13}$

The experimental testing has been conducted on an INSTRON (series IX) machine with machine parameters as follows:
Sample rate (pts/sec) : 20.00
Crosshead Speed (mm/min): 0.300

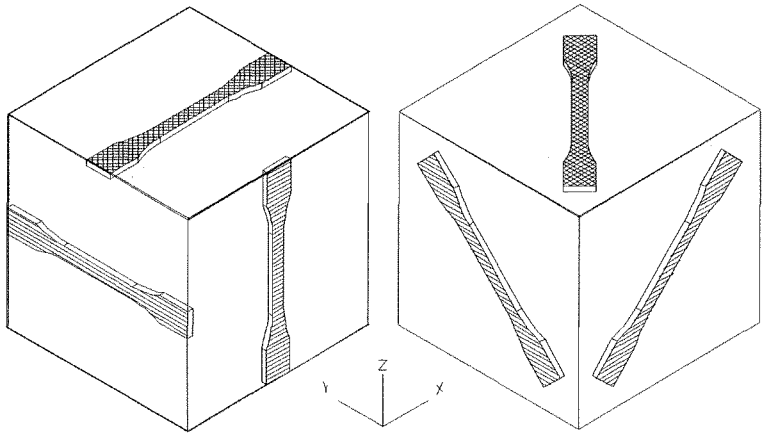

Figure 5: Tensile test specimen's orientation.

Figure 5 above shows orientation of tensile bars. The properties of these parts were found to be dependent mostly on the bar's orientation as compared to bar's individual layer lay-up and is evident from Table 1.

Bar No.	Build Plane	Orientation	Uni-directional Specimens [0°]		Quasi-Isotropic Specimens [0/90/45/-45]	
			Avg. tensile strength, MPa*	Avg. elastic modulus, MPa*	Avg. tensile strength, MPa**	Avg. elastic modulus, MPa**
1	xy	x	***	***	11.7	1072.90
2	yz	y	6.554	371.40	15.987	1652.523
3	xz	z	6.459	352.57	7.608	1391.448
4	xy	x+45	1.945	189.57	10.808	970.944
5	yz	y+45	5.605	295.1	13.465	1519.115
6	xz	z+45	6.231	300.83	14.702	1527.60

Table 1: Tensile tests results, Quasi-isotropic results from [3]

(*) Tests were performed at 0.3 mm/s crosshead speed
(**) Tests were performed at 5 mm/s crosshead speed
(***) Bar no. 1 was very weak and broke while loading it in the machine

As seen from Table 1, for the bars 2 and 3, average properties are high for yz-build plane both for uni-directional and quasi-isotropic specimens. This shows that parts with relatively shorter traverse length (corresponding to fiber length) have higher value for elastic modulus and tensile strength. This maybe because with longer traverse length, the likelihood of failure-inducing surface cracks increases. It must be noted here that loads applied were transverse to the roads for the two bars. A bar built in xz plane and oriented and tested along x-axis showed better tensile strength than bar 3. For the bars oriented at 45° to the axis, average elastic modulus is high for xz-build plane both for uni-directional and quasi-isotropic specimens. This shows that build direction strongly affects the part's strength irrespective of the stacking sequence. But the quasi bars are stronger than uni-directional bars as the total volume of voids in a particular

direction decreases because of the cross ply arrangement. The significant difference in values can be attributed to high difference in tensile testing speed of both the sets of bars.

Results:

Results of thermal expansion experiments are presented in table 2 and table 3.

	α xy [m/m-K]	α yz [m/m-K]	α xz [m/m-K]
Experiment 1 : heating	7.636E-05	7.561E-05	7.021E-05
cooling	8.939E-05	9.726E-05	9.621E-05
Experiment 2 : heating	9.181E-05	9.246E-05	8.871E-05
cooling	9.732E-05	9.795E-05	9.687E-05
Experiment 3 : heating	9.326E-05	9.440E-05	9.233E-05
cooling	9.693E-05	9.720E-05	9.648E-05

Table 2: Expansion coefficients for Quasi-Isotropic plates

	α xy [m/m-K]	α yz [m/m-K]	α xz [m/m-K]
Experiment 1 : heating	5.872E-05	3.570E-05	6.984E-05
cooling	7.843E-05	5.249E-05	8.335E-05
Experiment 2 : heating	7.368E-05	5.181E-05	7.698E-05
cooling	7.836E-05	5.289E-05	8.326E-05
Experiment 3 : heating	7.873E-05	5.529E-05	8.260E-05
cooling	7.864E-05	5.251E-05	8.368E-05

Table 3: Expansion coefficients for Uni-directional plates

It can be observed that the values of the Coefficient of Thermal Expansion (CTE) for the cooling portion of the experiments are higher than the heating values for both plates. CTE values for quasi plates are almost similar in all the three directions showing uniform expansion. CTE values for quasi plates are higher than those for uni directional plates, showing that there is more interfacial contact because of the cross-ply arrangement. The general trend shows that for uni-directional bars, yz orientation has lowest and xz orientation has highest CTE values. This is assumed to be related to the larger interface between roads normal to the build plane as compared to a smaller interfacial contact area in the build plane.

Experimental verification of laminate theory for FDM bars was done by comparing measured deformations with those predicted from the laminate theory. Alternatively, the compliances can be compared, an approach used in [7]. The measured normal strains on the upper surface (z = -t/2) are related to midplane strains and curvatures by

$$\varepsilon_x(u) = \varepsilon_x(0) - (t/2)\kappa_x$$
$$\varepsilon_y(u) = \varepsilon_y(0) - (t/2)\kappa_y$$

For a uniaxial loading test of such a strain-gaged specimen, compliances can be determined as follows

$$A'_{11} = \frac{\varepsilon_x(0)}{N_x} \qquad A'_{12} = \frac{\varepsilon_y(0)}{N_x} \qquad \text{and so on.}$$

Results were as follows,

A'_{11} = 4.6469E-01 1/MPa-m as predicted by laminate theory, while
A'_{11} = 4.4880E-01 1/MPa-m as measured by strain gage and equal to $\varepsilon_x(0)/N_x$.

Using E_{11}, E_{22}, E_{33}, ν_{12}, ν_{13}, ν_{23}, G_{12}, G_{23}, G_{13} as determined experimentally for Uni-directional bar, stiffness matrix was calculated using laminate theory with two ply sequences, viz. $[0]_{20}$ and $[0/90/45/-45]_{20}$.

For $[0]_{20}$ laminate, stiffness matrix was found to be,

$$[S] = \begin{bmatrix} 0.4024 & 0.22694 & 0.22696 & 0.0000 & 0.0000 & 0.0000 \\ 0.22694 & 0.63790 & 0.39376 & 0.0000 & 0.0000 & 0.0000 \\ 0.22696 & 0.39376 & 0.60557 & 0.0000 & 0.0000 & 0.0000 \\ 0.0000 & 0.0000 & 0.0000 & 0.1189 & 0.0000 & 0.0000 \\ 0.0000 & 0.0000 & 0.0000 & 0.0000 & 0.2190 & 0.0000 \\ 0.0000 & 0.0000 & 0.0000 & 0.0000 & 0.0000 & 0.0799 \end{bmatrix} \text{ GPa}$$

For $[0/90/45/-45]_{20}$ laminate, stiffness matrix was found to be,

$$[S] = \begin{bmatrix} 0.4809 & 0.26615 & 0.31036 & 0.0000 & 0.0000 & 0.0000 \\ 0.26615 & 0.48053 & 0.31000 & 0.0000 & 0.0000 & 0.0000 \\ 0.31036 & 0.3100 & 0.60534 & 0.0000 & 0.0000 & 0.0000 \\ 0.0000 & 0.0000 & 0.0000 & 0.1518 & 0.0000 & 0.0000 \\ 0.0000 & 0.0000 & 0.0000 & 0.0000 & 0.1518 & 0.0000 \\ 0.0000 & 0.0000 & 0.0000 & 0.0000 & 0.0000 & 0.1070 \end{bmatrix} \text{ GPa}$$

As E_{11} value of the uni-directional bar was less than E_{22} value, we see that S_{11} term for quasi plate is higher than S_{11} term of 0° plate. It can be also seen from the fact that S_{22} term is higher than S_{11} term of 0° plate.
As compared to the stiffness matrix determined by laminate theory for quasi-isotropic lay-up (using the properties from the tensile test of uni-directional bars), the actual stiffness matrix of quasi laminate (using the properties from the tensile tests of quasi bars) was found to be (as given in [3]),

$$[S] = \begin{bmatrix} 1.8530 & 1.4348 & 1.1810 & 0.0000 & 0.0000 & 0.0000 \\ 1.4348 & 3.0843 & 1.6444 & 0.0000 & 0.0000 & 0.0000 \\ 1.1810 & 1.6444 & 2.4141 & 0.0000 & 0.0000 & 0.0000 \\ 0.0000 & 0.0000 & 0.0000 & 0.5540 & 0.0000 & 0.0000 \\ 0.0000 & 0.0000 & 0.0000 & 0.0000 & 0.5405 & 0.0000 \\ 0.0000 & 0.0000 & 0.0000 & 0.0000 & 0.0000 & 0.3696 \end{bmatrix} \text{ GPa}$$

It can be seen that although there is significant difference in values, both matrices show almost similar behavior among their 44, 55 and 66 terms. G_{12} value for quasi bar is higher than that of the uni-directional bar showing that roads with $\pm 45°$ orientation will be most effective in carrying shear loads.

The difference in values can be accounted to the low modulus values of uni-directional bars. Two reasons can be given for the high difference in stiffness values of the two sets of bars: first, strain gages were used with a different data acquisition method and second, the tensile tests were carried out at a lower testing speed than those for quasi isotropic bars.

Conclusion:

It is obvious that better mechanical properties could be achieved from any FDM part by selecting a particular build orientation depending on the direction of load application in service and part geometry. The results of the experimental work conducted will provide a useful guideline to the user before building a FDM part.

The current low strength values of the parts can be improved by developing better toolpaths. This along with previous work done on surface finish (which is shown to depend on layer thickness and also orientation) will provide a useful tool in building an overall very good quality FDM part.

References:

[1]. Analog Devices, "AD594/AD595 Monolithic Thermocouple Amplifiers with Cold Junction Compensation", Technical Note, 1997.

[2]. Analog Devices, "AD624, Precision Instrumentation Amplifier", Technical Note, 1996.

[3]. M. Bertoldi, M. A. Yardimci, C. Pistor, S. I. Güçeri, "Mechanical Characterization of Parts Processed via Fused Deposition", Proceedings of the 1998 Solid Freeform Fabrication Symposium, Austin, TX, 1998.

[4]. Measurements Group, "Measurement of Thermal Expansion Coefficient", Measurements Group Tech Note TN-513-1, 1994.

[5]. TA Instruments, "Modulated DSC® (MDSC®): How Does It Work?" http://www.tainst.com/media/mdsc.pdf , 1999.

[6]. Yardimci, M.A., "Process Analysis and Planning for Fused Deposition", Ph.D. Thesis, Department of Mechanical Engineering, University of Illinois at Chicago, 1999.

[7]. Tsai, S.W., "Structural Behavior of Composite Materials", NASA CR-71 1964.